SAND2013-6683C
Proceedings of the Australian Combustion Symposium
November 6-8, 2013, The University of Western Australia

Structural transitions of lifted laminar dimethyl ether flames with temperature variation

A. Krisman[1, *], E.R. Hawkes[1,2], M. Talei[1], A. Bhagatwala[3], J.H. Chen[3]
[1]School of Mechanical and Manufacturing Engineering
University of New South Wales, NSW 2019 Australia
[2]School of Photovoltaic and Renewable Energy Engineering
University of New South Wales, NSW 2019 Australia
[3]Sandia National Laboratories, Combustion Research Facility
Livermore, California, CA 94551, United States of America

Abstract

A direct numerical simulation parametric study of laminar, two-dimensional dimethyl ether jet flames in heated co-flow was conducted at a pressure of 40 atmospheres by varying the co-flow temperature. Four cases were considered at co-flow temperatures of 900, 1100, 1300, and 1500 K. The temperatures were selected to produce a transition from within the negative temperature coefficient (NTC) regime to beyond it. New flame structures are observed in all cases. The flames have a modified edge-flame structure at 900 and 1100 K. In addition to a tribrachial edge-flame, there is a fourth heat release branch upstream of the stabilisation point associated with the low temperature kinetics, as such these cases exhibit a tetrabrachial structure. At 1300 K, the flame autoignites and has a tribrachial structure immediately downstream of the stabilisation point in addition to two heat release branches upstream, one at very lean mixture fractions leading to autoignition and the other at rich mixture fractions associated with the low temperature kinetics, giving the flame a pentabrachial structure. At 1500 K, the low temperature kinetics and heat release branch are not observed and the flame reverts to a tetrabrachial structure that is qualitatively different to the 900 and 1100 K cases.

Keywords: DNS, dimethyl ether, tribrachial flame, triple flame, autoignition, negative temperature coefficient

1. Introduction

Lifted jet flames are an archetypal flame that are observed in practical combustors, for example, in diesel engines. Additionally, lifted jet flames exhibit complex turbulence-chemistry interactions and present a substantial challenge for model prediction in computational fluid dynamics. For this reason, substantial effort has been applied using experimental, numerical, and theoretical tools to gain insight [1, 2].

In this study, a direct numerical simulation (DNS) approach was applied to a diesel-like fuel at realistic engine temperature and pressure. In order to perform the DNS, important diesel phenomena were neglected due to computational constraints. Turbulence, multiphase flow, sooting processes and radiative heat transfer, multi-jet injection, and transient effects were all neglected. In doing so, the study focused on the interactions between the fuel chemistry and the shearing, nonpremixed laminar jet.

Previous DNS studies in a mixing layer configuration [3, 4] showed propagating tribrachial edge-flame solutions. However, no DNS studies of similar flames have been performed at diesel-like thermo-chemical environment in a jet configuration using a fuel capable of reproducing the multi-stage ignition and the low temperature chemical kinetics of diesel fuel. In the context of diesel-like conditions the edge-flame may affect the lift-off height, which is an important parameter that controls fuel-air mixing and hence pollutant formation, so a DNS study at diesel-like conditions provides underlying physical insight.

Dimethyl ether (DME), was selected as one of the simplest oxygenated ethers with diesel fuel characteristics of multi-stage ignition and high cetane number. The 30 species DME chemical mechanism used in this study was provided by Lu et al. (personal communication) [5]. The chemical mechanism was obtained by a reduction of the detailed mechanism developed by Zhao et al. [6] using reduction methods outlined by Lu and Law [7].

Like diesel fuel, DME exhibits two-stage ignition. Due to a transition between low-temperature and high-temperature chemical pathways, it exhibits a non-monotonic relationship between ambient temperature and ignition delay time. This produces a negative temperature coefficient (NTC) regime, where increasing the ambient temperature results in prolonged ignition delay times [6, 8]. At a pressure of 40 atm, DME exhibits NTC behaviour for ambient temperatures in the range of approximately 800 to 1100 K [9].

This study investigates moderate to highly heated co-flow temperatures of 900, 1100, 1300, and 1500 K. Zero-dimensional homogeneous ignition delay simulations over this temperature range show a transition from long to short ignition delay times, corresponding to a transition from NTC to non-NTC regimes.

The DNS is performed using a fully parrallelised code, S3D [10], which solves the compressible Navier-Stokes and species-conservation equations using a high order, low-dissipation spatial finite difference method combined with an explicit Runge-Kutta time advancement.

* Corresponding author: Alexander Krisman
Phone: (+61) 431 912 920
Email: a.krisman@unsw.edu.au

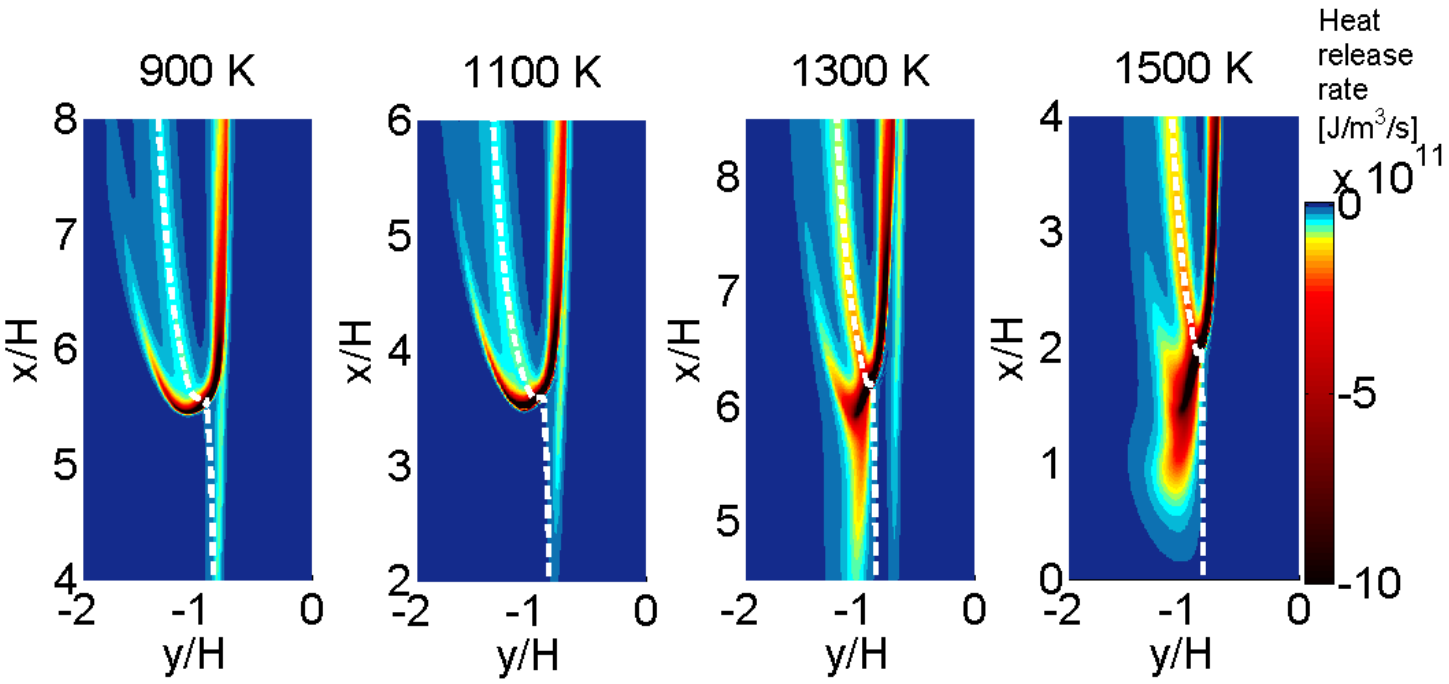

Figure 1: Domain coloured by heat release rate. Stoichiometric mixture fraction marked by dashed white line.

2. Configuration

The computational configuration is a two-dimensional planar lifted laminar DME jet flame in a heated air co-flow at an elevated pressure of 40 atm. The Cartesian mesh domain consisted of a two-dimensional grid. In the stream-wise direction, x, a diluted planar fuel jet consisting of 70% DME and 30% N_2 (by volume) issues into an oxidising environment comprised of 79% N_2 and 21% O_2. The x inlet is a hard inflow boundary condition and a non-reflecting outflow condition is imposed at the x outlet. The jet is located at the right boundary in the y direction where a plane of symmetry is imposed. The left y boundary corresponds to a non-reflecting outflow. The boundary conditions are imposed using the Navier-Stokes characteristic boundary condition (NSCBC) method [11] with transverse terms evaluated on the stream-wise outflow boundary as in Yoo *et al.* [12].

The domain size is 10 jet heights in the x direction and 5 jet heights in the y direction for all simulations, where the jet height is H = 0.3 (mm). The velocity of the jet and the co-flow are varied to produce a stabilised flame within the computational domain and to maintain a fixed velocity deficit, U_{JET}-U_{COFLOW} = 17.5 (m/s), maintaining a constant shear rate between the cases.

The computational domain consisted of a stretched Cartesian grid. For the 900 K case, a grid spacing of 1.25 microns was required in the vicinity of the stabilisation point to resolve the thin flame structures. For all other cases, a grid spacing of 2.5 microns was sufficient. The integrating time step was determined by the acoustic CFL limit and imposed a time step of 0.5 nano seconds for the 900 K case and 1.0 nano seconds for the other cases. Table 1 presents the key physical parameters for each case.

Table 1: Key parameters for each case.

Parameter	Unit	900K	1100K	1300K	1500K
U_{JET}	m/s	20.0	21.0	26.5	55.5
U_{COFLOW}	m/s	2.5	3.5	9.5	48.0
T_{JET}	K	400	400	400	400
T_{COFLOW}	K	900	1100	1300	1500
Pressure	Atm.	40	40	40	40
Δx (min)	μm	1.25	2.5	2.5	2.5

3. Results

Figure 1 shows the heat release rate fields for the 4 cases, with the stoichiometric mixture fraction (Z=0.123) line superimposed. All cases have a stabilised flame.

The 900 K case shows a new kind of edge-flame structure at the stabilisation point which to the best of our knowledge has not been previously observed. The flame consists of four branches and will be termed a tetrabrachial flame. The main flame resembles a conventional tribrachial edge flame with central crescent-shaped rich and lean premixed flames and a trailing diffusion flame. This edge flame is centered about the stoichiometric mixture fraction which corresponds to a stream-wise velocity comparable to the co-flow. The propagation speed of the flame is matched by the local fluid velocity which is diminished compared to the free-stream velocity due to flow redirection about the flame-base (not shown here). However, upstream of the tribrachial flame, an additional branch of heat release is observed. The upstream heat release originates from very lean mixture fractions (not shown here), and moves to rich mixture fractions just upstream of the tribrachial flame, see the left-most plot in Fig. 1. This heat release branch is associated with the first stage of ignition and low temperature kinetics. The low temperature heat

release moves to richer mixture fractions further downstream, eventually merging with the rich branch of the tribrachial flame just beyond the stabilisation point.

The 1100 K case resembles the 900 K case. The major difference is the diminishment of the low temperature heat release. It does not occur until further downstream compared to the 900 K case and is reduced in magnitude. The tribrachial flame is still observed as the stabilisation mechanism.

At 1300 K, a transition from edge flame propagation to auto-ignition is observed. Originating from extremely lean mixture fractions, the heat release leading to autoignition occurs over multiple jet heights. A main tribrachial flame structure is still apparent immediately downstream of the autoignition location. However, upstream of the tribrachial flame there are now two distinct additional branches: a strong heat release region on the lean side and a weaker heat release region on the rich side, making the flame at this condition pentabrachial. The branch on the lean side is a result of high temperature, single-stage ignition. The branch on the rich side is the result of the low temperature heat release, as observed in the 900 and 1100 K cases, but further diminished in magnitude and shifted to richer mixture fractions.

At 1500 K, the auto-ignition becomes stronger and confined to a smaller region of space. The low temperature chemistry upstream of the stabilisation point is no longer observed.

The heat release behaviour upstream of the stabilisation point can be understood by considering a zero-dimensional solution to the chemical mechanism. The solver SENKIN (which is part of the CHEMKIN-III suit [13]) was used to produce a set of constant pressure simulations of the DME fuel over a range of initial oxidiser temperatures and mixture fractions at a fixed pressure and fuel composition. The results are presented in Fig. 2.

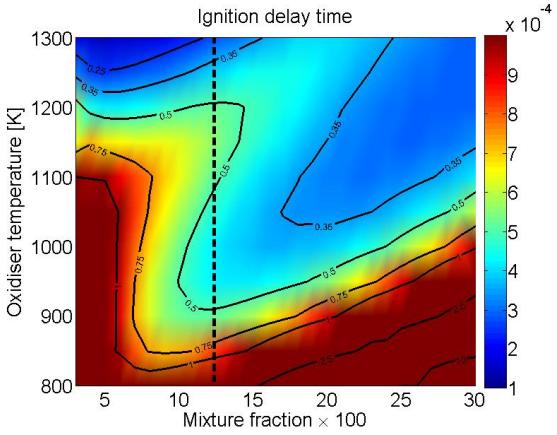

Figure 2: Map of ignition delay times by initial oxidiser temperature and mixture fraction at a pressure of 40 atmospheres and a fuel diluted with 30% N_2. The bold, dashed line marks the stoichiometric mixture fraction. The colour shading is in units seconds and the contours are in units milliseconds.

As can be seen in Fig. 2, there are two distinct regimes of local minima of the ignition delay time. From 900 to 1100 K, the most reactive mixture fraction (the mixture fraction having the shortest ignition delay) shifts from lean to rich with increasing temperature. This corresponds to the movement of the low temperature heat release branch towards the jet centre at 1100 K, compared to the 900 K case. At approximately 1250 K the minimum ignition delay time shifts as a jump-discontinuity to extremely lean mixture fractions. This transition was correlated with the flame-to-autoignition transition observed in the 1300 K case. At this temperature, the flame is stabilised by autoignition which is initiated from very lean mixture fractions far upstream of the stabilization point (not shown here). At 1300 K, the low temperature heat release is still observed, but closer to the jet center at very rich mixture fraction values.

Figure 3 shows the vicinity of the stabilisation point for all simulations. Heat release rate and minor species mass fractions are presented to compare the flame characteristics between the four cases.

The OH mass fraction, Y_{OH}, is selected as a marker of high temperature heat release and reveals the strongest signature about the stoichiometric line which coincides with the trailing nonpremixed flame behind the stabilisation point. The ethylene mass fraction, Y_{C2H4}, clearly shows the difference between the edge-flame and autoignition cases. In the 900 and 1100 K cases, ethylene marks the lean and rich premixed branches of the edge-flame. In the 1300 and 1500 K cases, ethylene also reveals the region of heat release associated with autoignition. The mass fraction of methoxymethyl-peroxy radical, $Y_{CH3OCH2O2}$, was selected as the marker for the low temperature chemistry. The species was selected as it is involved in a chain branching reaction critical to the low temperature heat release pathway, and is also involved in a reaction that inhibits the "hot" ignition of the flame [6]. The results show that the low temperature chemistry is reduced when the co-flow temperature is increased and by the 1500 K case there is no low temperature chemistry apparent.

4. Conclusions

With a view to understanding the possible importance of edge flames in lifted flame stabilisation in diesel engines, a set of laminar edge flame DNS has been carried out in engine-relevant thermo-chemical conditions. At the considered conditions, the mixture ahead of the edge flame can autoignite, which introduces different behaviours compared with edge flames at atmospheric conditions.

A parametric study varying the ambient temperature was conducted to observe a range of different possible behaviours. Four cases were considered at 900, 1100, 1300, and 1500 K at a fixed pressure of 40 atm.

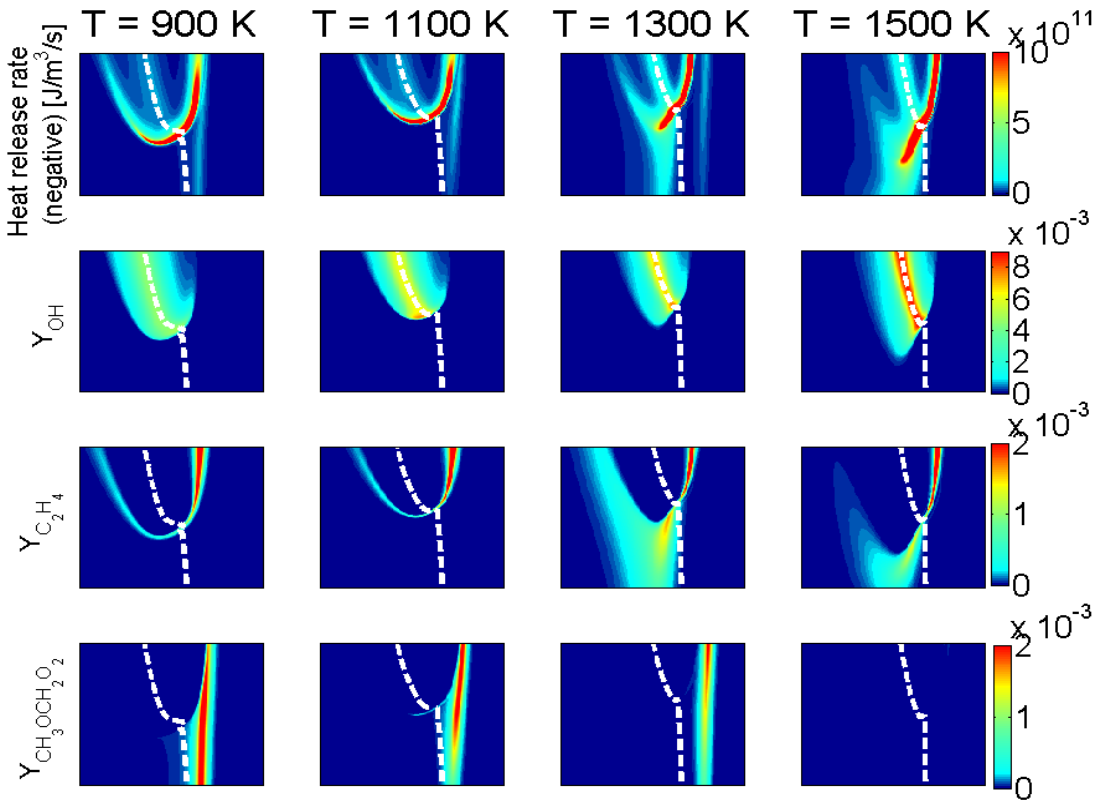

Figure 3: Stabilisation point coloured by heat release rate, OH mass fraction, C_2H_4 mass fraction, and $CH_3OCH_2O_2$ mass fraction from the top to the bottom row. Columns from left to right represent each case in order of increasing co-flow temperature. Each subplot is a 2-H by 2-H window centered about the stabilisation point for each simulation. The white dashed line shows the stoichiometric mixture fraction.

For all cases, new flame structures were observed. All of the flames exhibited a tribrachial main flame structure similar to that observed at atmospheric conditions, with a crescent-shaped premixed combustion region and a trailing diffusion flame. However, unlike edge flames in atmospheric conditions, the flames exhibited additional upstream branches such that the flames were tetrabrachial or pentabrachial.

For the 900K and 1100K conditions, the upstream branch was located on the rich side in the vicinity of the stabilisation point and resulted from the first stage of the two-stage ignition process and low-temperature chemical kinetic pathways. At 1500K, the upstream branch was located on the lean side and was the result of high temperature, single stage autoignition. At the intermediate temperature of 1300K, both low and high temperature branches were evident.

The stabilisation mechanism was found to be temperature dependent, with the higher temperature flames propagating at high velocity and being stabilised essentially by autoignition while at the lower temperature conditions the velocity was more modest and the flame appeared to be stabilised by premixed flame propagation.

The results suggest that even in autoignitive conditions, essentially premixed edge-flame structures or hybrid premixed-autoignition structures can occur, and these could therefore be involved with the stabilisation of lifted flames in diesel engines. Further work is needed to understand how such structures are affected by a number of parameters including velocity, mixing layer thickness, shear, and turbulence.

5. Acknowledgements

This work was supported by the Australian Research Council (ARC). The work at Sandia National Laboratories was supported by the Division of Chemical Sciences, Geosciences and Biosciences, the Office of Basic Energy Sciences, the US Department of Energy (DOE). The research was also supported by computational resources on the Australian NCI National Facility through the National Computational Merit Allocation Scheme and Intersect Australia partner share.

6. References

[1] K.M. Lyons, Prog. Energ. Combust., **33** (2) (2007), pp. 211-231.

[2] C.J. Lawn, Prog. Energ. Combust., **35** (2009), pp. 1-30.

[3] T. Echekki, H. Chen, Combust. Flame, **114** (1997), pp. 231–245.

[4] H.G. Im, J.H. Chen, Combust. Flame, **119** (1999), pp. 436–454.

[5] T.F. Lu, Personal communication (2012).

[6] Z. Zhao, M. Chaos, A. Kazakov, F. Dryer, Int. J. Chem. Kinet. **40** (1) (2007), pp. 1–18.

[7] T.F. Lu, C.K. Law, Prog. Energ. Combust. **35** (2) (2009), pp. 192-215.

[8] H. J. Curran, S. L. Fischer, F. L. Dryer, Int. J. Chem. Kinet. **32** (12) (2000), pp. 741-759.

[9] P. Dagaut, C. Daly, J.M. Simmie, M. Cathonnet, Proc. Combust. Inst. **27** (1998), pp. 361-369.

[10] J.H. Chen, A. Choudhary, B. de Supinski, M. DeVries, E.R. Hawkes, S. Klasky, W.K. Liao, K.L. Ma, J. Mellor-Crummey, N. Podhorszki, R. Sankaran, S. Shende, C.S. Yoo, Comput. Sci. Disc. **2** (2009), pp. 015001.

[11] T. Poinsot, S.K. Lele, J. Comput. Phys. **101** (1992), pp. 104-129.

[12] C. S. Yoo, Y. Wang, A. Trouvé, H. G. Im, Combust. Theor. Model. **9** (4) (2005), pp. 617-646.

[13] Lutz A.E., Kee R.J., Miller J.A.. Sandia National Laboratories Report No. SAND87-8248; 2002.